1590 *Biochemistry* **2010,** *49,* 1590–1595
DOI: 10.1021/bi901881c

BIOCHEMISTRY
including biophysical chemistry & molecular biology
Article

DNA Bending by the Mammalian High-Mobility Group Protein AT Hook 2†

Bo Chen, Jasmine Young, and Fenfei Leng*

Department of Chemistry and Biochemistry, Florida International University, 11200 SW 8th Street, Miami, Florida 33199

Received November 3, 2009; Revised Manuscript Received January 7, 2010

ABSTRACT: The mammalian high-mobility group protein AT hook 2 (HMGA2) is a DNA binding protein that specifically recognizes the minor groove of AT-rich DNA sequences. Disruption of its expression pattern is directly linked to oncogenesis and obesity. In this paper, we constructed a new plasmid pBendAT to study HMGA2-induced DNA bending. pBendAT carries a 230 bp DNA segment containing five pairs of restriction enzyme sites, which can be used to produce a set of DNA fragments of identical length to study protein-induced DNA bending. The DNA fragments of identical length can also be generated using PCR amplification. Since pBendAT does not contain more than three consecutive AT base pairs, it is suitable for the assessment of DNA bending induced by proteins recognizing AT-rich DNA sequences. Indeed, using pBendAT, we demonstrated that HMGA2 is a DNA bending protein and bends all three tested DNA binding sequences of HMGA2, SELEX1, SELEX2, and PRDII. The DNA bending angles were estimated to be 34.2°, 33.5°, and 35.4°, respectively.

The mammalian high-mobility group protein AT hook 2 (HMGA2)[1] is a transcriptional factor involved in mesenchymal cell differentiation and transformation (*1*−*3*). It plays an important role in fat cell proliferation (*2*) and is considered to be a potential target for the treatment of obesity (*2*, *4*). HMGA2 is also an oncoprotein associated with the formation of a variety of tumors, including benign tumors, such as uterine leiomyomas (*5*), lipomas (*6*, *7*), and pulmonary chondroid hamartomas (*8*), and malignant tumors, such as lung cancers (*9*−*11*), breast cancers (*12*), and leukemia (*13*). Interestingly, the expression level of HMGA2 was demonstrated to be correlated with the degree of malignancy, the existence of metastasis, and a poor prognosis for certain cancers (*14*, *15*). These results suggest that HMGA2 is a potential target for treatment of these cancers (*4*, *16*, *17*).

HMGA2 is a DNA binding protein containing three AT hook DNA binding domains that specifically recognize the minor groove of AT-rich DNA sequences (*18*). Although each AT hook DNA binding domain binds to five AT base pairs (*18*, *19*), the high-affinity binding of HMGA2 requires two to three appropriately spaced 5 bp AT-rich DNA sequences as a single multivalent binding site (*20*). The DNA binding constant of multivalent binding is much greater than that of single valent binding (*21*). Previously, using a PCR-based systematic evolution of ligands by exponential enrichment (SELEX) procedure, we identified two consensus sequences for HMGA2: 5′-ATATTCGCGAWWATT-3′ or 5′-ATATTGCGCAWWATT-3′, where W is A or T (*21*). Our results showed that the three segments in the consensus sequences (two AT-rich segments and one GC-rich segment) are required for high-affinity binding; mutations of these sequences significantly reduced the DNA binding affinity of HMGA2. These results indicate that HMGA2 does not randomly recognize any AT-rich sequences. In contrast, it binds to specific AT-rich DNA sequences (*21*).

Here we decided to study HMGA2-induced DNA conformational change, specifically DNA bending. Since each AT hook DNA binding domain contains five to six positive charges, it should bend the DNA locus upon binding to the AT-rich DNA sequences (*22*). The challenge is to find a short DNA fragment that does not contain four or five consecutive AT base pairs for the gel permutation assay. In this case, we can clone one HMGA2 binding site into this short DNA fragment and precisely determine the HMGA2-induced DNA bending angle without the interference caused by HMGA2 binding to other AT-rich sequences, i.e., sequences containing more than three consecutive AT base pairs. In this study, we constructed a new plasmid pBendAT to study HMGA2-induced DNA bending. pBendAT carries a 230 bp DNA sequence that does not contain more than three consecutive AT base pairs and therefore does not have an AT-rich sequence. It also contains five pairs of restriction enzyme recognition sites that can be used to generate a set of DNA fragments of identical length for studying DNA bending. Using this new plasmid, we demonstrated that HMGA2 bends all three binding sites of HMGA2, SELEX1, SELEX2, and PRDII [positively regulatory domain II of human interferon-β enhancer (*23*); HMGA2 was previously demonstrated to bind to PRDII and increase transcription activities mediated byNF-κB (*24*)].

MATERIALS AND METHODS

Protein and Synthetic Deoxyoligonucleotides. The mammalian high-mobility group protein AT hook 2 (HMGA2) was expressed and purified as described previously (*19*, *25*). An extinction coefficient of 5810 cm^{-1} M^{-1} was used to determine the HMGA2 concentration. Synthetic deoxyoligonucleotides were purchased from MWG-Biotech, Inc. (High Point, NC).

Plasmids. Plasmid pBend2 is a generous gift of S. Adhya (National Institutes of Health, Bethesda, MD). Plasmid

†F.L. acknowledges Grant 1SC1HD063059-01A1 from the National Institutes of Health (to F.L.) and Grant 08BB-11 from State of Florida Department of Health (to A. McGoron and F.L.).

*To whom correspondence should be addressed: Department of Chemistry and Biochemistry, Florida International University, 11200 SW 8th St., Miami, FL 33199. Telephone: (305) 348-3277. Fax: (305) 348-3772. E-mail: lengf@fiu.edu.

[1]Abbreviations: HMGA2, mammalian high-mobility group protein AT hook 2; EMSA, electrophoretic mobility shift assay; nt, nucleotides.

 Published on Web 01/28/2010

Table 1: Deoxyoligonucleotides Used To Construct Plasmid pBend-AT

name	length (bp)	DNA sequence
FL423	70	5′-GAATTCTCCGGACTCGTCGTCCTGGCGGTACCACGCTATCTGTGCAAGGTGCTAGCCACCGGACACGTGC-3′
FL424	70	5′-GCCGGTCGACTCTAGAGAGCTCCTTCACCTCGGTGGTGGACACTCGGATCCTGGAGCACGTGTCCGGTGG-3′
FL425	70	5′-GCTCTCTAGAGTCGACCGGCCGCACCAGGTCAACAGGCATGCACCGGCCTCTTCATGCGACCTAGGAGCG-3′
FL426	70	5′-AAGCTTCTGCAGTACTTCCCGTCCTCCAGAGGGACAGATCTGCGATGCTGAAGGTCGCTCCTAGGTCGCA-3′
FL427	21	5′-CCAGAATTCTCCGGACTCGTC-3′
FL428	20	5′-GCCGGTCGACTCTAGAGAGC-3′
FL429	20	5′-GCTCTCTAGAGTCGACCGGC-3′
FL430	22	5′-ACCAAGCTTCTGCAGTACTTCC-3′

pBendAT was constructed by the insertion of a 230 bp PCR product into the EcoRI and HindIII sites of pBend2. The 230 bp PCR product was created in two steps using synthetic deoxyoligonucleotides FL423, FL424, FL425, FL426, FL427, FL428, FL429, and FL430 (Table 1). The first step was to make two 125 bp PCR fragments: one using FL423 and FL424 with 15 bp of overlapping DNA sequence as the DNA templates and FL427 and FL428 as the primers and another one using FL425 and FL426 with 15 bp of overlapping DNA sequence as the DNA templates and FL429 and FL430 as the primers. The second step was to create the 230 bp PCR fragment using the two 125 bp PCR fragments with 20 bp of overlapping DNA sequence as the DNA template and FL427 and FL430 as the primers. The map of pBendAT and the DNA sequence of the 230 bp PCR product are shown in Figure 1. Plasmids pBend2-CRP, pBend2-SELEX1, pBend2-SELEX2, pBend2-PRDII, pBendAT-CRP, pBendAT-SELEX1, pBendAT-SELEX2, and pBendAT-PRDII were created by the insertion of a synthetic XbaI DNA fragment containing a CRP binding site or a HMGA2 binding site into the unique XbaI site of pBend2 or pBendAT, respectively. Table 2 summarizes the main properties of these plasmids. All DNA elements were confirmed by DNA sequencing.

Determination of the Protein-Induced DNA Bending Angle. Plasmid pBendAT derivatives containing a CRP binding site or a HMGA2 binding site (Table 2) were digested by a pair of restriction enzymes, BspEI and EagI, KpnI and SphI, NheI and AvrII, BamHI and BglII, and SacI and PstI, to produce a set of fragments with identical length and base composition in which the position of the protein binding site is variable. Alternatively, these DNA fragments were produced using polymerase chain reaction using primers shown in Figure 2. We also used pBend2 derivatives to generate a set of fragments with identical length and base composition in which the position of the protein binding site is variable after they have been digested with restriction enzymes MluI, NheI, EcoRV, SspI, and BamHI. The DNA fragments were labeled with ^{32}P at 5′-termini by T4 polynucleotide kinase in the presence of [γ-^{32}P]ATP. The protein−DNA complexes were formed by addition of 2.0−20.0 $\times$ 10^{-9} M protein to a solution containing 2 $\times$ 10^{-10} M ^{32}P-labeled DNA. After equilibration for 60 min at 22 °C, the samples were loaded onto a polyacryamide gel to determine the mobility of protein−DNA complexes, which is dependent upon the position of the bound protein, with the lowest mobility present when the protein is bound to the center of the fragment. The bending angle α by which the DNA is bent from linearity was estimated by

$$\cos\left(\frac{\alpha}{2}\right) = \frac{\mu_M}{\mu_E} \quad (1)$$

where μ_M and μ_E are the mobility of the complex with protein bound at the center and the end of DNA, respectively (*26*).

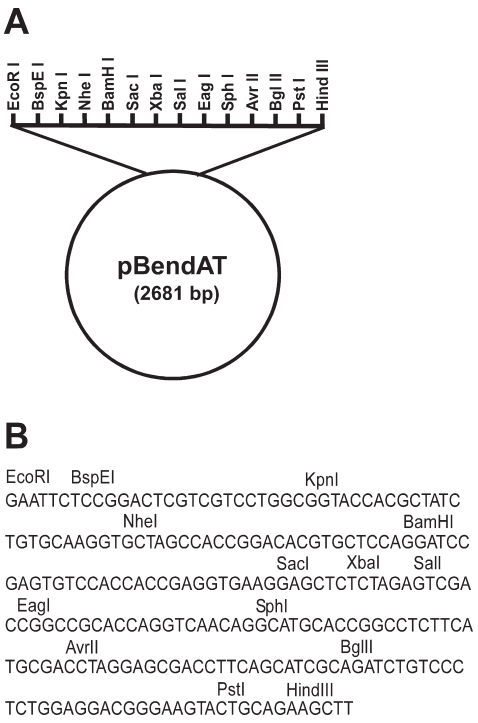

FIGURE 1: (A) Map of plasmid pBendAT. (B) Nucleotide sequence of the 230 bp fragment of pBendAT between the EcoRI and HindIII sites. The restriction enzyme sites for EcoRI, BspEI, KpnI, NheI, BamHI, SacI, XbaI, SalI, EagI, SphI, AvrII, BglII, PstI, and HindIII are shown.

Table 2: Plasmids Constructed during This Study

plasmid	DNA binding site	DNA binding sequence (top strand)
pBend2-CRP	CRP binding site	5′-TAATGTGAGT-TAGCTCACTCAT-3′
pBendAT-CRP	CRP binding site	5′-TAATGTGAGTTA-GCTCACTCAT-3′
pBend2- SELEX-1	SELEX1	5′-ATATTCGCGATTATT-3′
pBendAT-SELEX-1	SELEX1	5′-ATATTCGCGATTATT-3′
pBend2- SELEX-2	SELEX2	5′-ATATTGCGCATTATT-3′
pBendAT-SELEX-2	SELEX2	5′-ATATTGCGCATTATT-3′
pBend2-PRDII	PRDII	5′-TCGACTGTAAATGAC-ATAGGAAAAC-3′
pBendAT-PRDII	PRDII	5′-TCGACTGTAAATGA-CATAGGAAAAC-3′

Electrophoretic Mobility Shift Assay (*EMSA*). DNA fragments containing a DNA binding site of one DNA binding protein (the NheI−-AvrII fragment of the pBendAT or EcoRV fragment of pBend2 derivatives) were labeled with ^{32}P at their

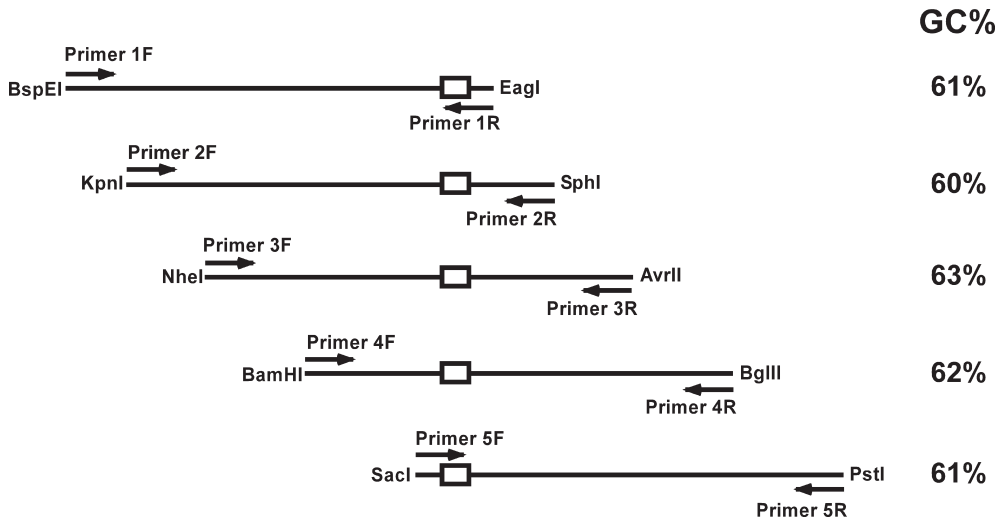

FIGURE 2: Five DNA fragments of identical length, which can be produced by restriction enzyme digestion or PCR amplification and used in the DNA bending experiments. The GC% values are also shown. The empty rectangle indicates the DNA binding site. The following are DNA sequences for the primers: primer 1F, 5′-TCGTCGTCCTGGCGGTAC-3′; primer 1R, 5′-GCGGCCGGTCGACTCTAG-3′; primer 2F, 5′-ACCACGCTATCTGTGCAA-3′; primer 2R, 5′-TGCCTGTTGACCTGGTGC-3′; primer 3F, 5′-AGCCACCGGACACGTGCT-3′; primer 3R, 5′-AGGTCGCATGAAGAGGCC-3′; primer 4F, 5′-TCCGAGTGTCCACCACCG-3′; primer 4R, 5′-TCTGCGATGCTGAAGGTC-3′; primer 5F, 5′-ACCGAGGTGAAGGAGCTC-3′; primer 5R, 5′-TCCAGAGGGACAGATCTG-3′.

5′-termini by T4 polynucleotide kinase in the presence of [γ-^{32}P]ATP. The protein−DNA complexes were formed by addition of appropriate amounts of the protein to a solution containing 0.2 nM ^{32}P-labeled DNA in the 1× DNA binding buffer consisting of 20 mM Tris-HCl (pH 8.0), 200 mM NaCl, 0.5 mM EDTA, 1 mM DTT, 5 mM $MgCl_2$, and 5% glycerol. After equilibration for 60 min at 22 °C, the samples were loaded on a 8% native polyacryamide gel in 0.5× TBE buffer [0.045 M Tris-borate (pH 8.3) and 1 mM EDTA] to separate free and bound DNA. The gels were subsequently dried and visualized by autoradiography or quantified using a Fuji FLA 3000 image analyzer. The radioactivity of the free and bound DNA was determined and used to calculate the binding ratio (R), which is equal to the ratio of the radioactivity of the bound DNA divided by the sum of the radioactivity of the bound and free DNA. The apparent DNA binding constant (K_{app}) was obtained by nonlinear least-squares fitting to the following equation using Scientist.

$$R = \frac{a + x + 1/K_{app} - \sqrt{(a+x+1/K_{app})^2 - 4ax}}{2a} \qquad (2)$$

where a and x represent the total DNA and total protein concentrations, respectively.

RESULTS AND DISCUSSION

Initially, we cloned a few HMGA2 binding sites, such as SELEX1, SELEX2, and PRDII [positive regulatory domain II of human interferon-β enhancer (*23*)], into the XbaI site of pBend2 to study DNA bending induced by HMGA2. However, we noticed that the 236 bp DNA sequence of pBend2, used to generate a set of circularly permuted fragments, contains multiple AT-rich DNA sequences that may bind to HMGA2 (Figure S1 of the Supporting Information) and therefore interfere with the determination of the DNA bending angle by HMGA2. Indeed, our gel mobility shift assay confirmed that HMGA2 binds to all these AT-rich DNA sequences (Figure S2 of the Supporting Information). In this case, pBend2 derivatives, i.e., pBend2-SELEX1, pBend2-SELEX2, and pBend2-PRDII, cannot be used to precisely determine HMGA2-induced DNA bending angles. In this study, we decided to construct another pBend plasmid, pBendAT, to study HMGA2-induced DNA bending. Our strategy was to create and clone a 230 bp DNA sequence that does not contain three consecutive AT base pairs, into EcoRI and HindIII sites of pBend2 (Figure 1). This 230 bp DNA sequence also contains five pairs of restriction enzyme recognition sites that can be used to generate a set of linear DNA fragments of identical length after they have been cleaved with the pair of restriction enzymes (Figure 2). In addition, this set of identically sized DNA fragments can be produced using polymerase chain reaction amplification (Figure 2). Since the GC contents of these DNA fragments are almost identical (Figure 2), their mobilities during electrophoresis are also identical (see below for detail). Figure 1 shows the map of pBendAT and the nt sequence of the 230 bp DNA sequence. Figure 2 shows the set of DNA fragments of identical length that can be generated from pBendAT by restriction digestion or PCR amplification.

Next, we cloned the CRP binding site of the *lac P1* promoter into the XbaI site of pBendAT to produce plasmid pBendAT-CRP (Table 2) and compared the CRP-induced DNA bending for the DNA fragments generated from plasmids pBend2-CRP and pBendAT-CRP. For pBendAT-CRP, a set of DNA fragments of identical size were also generated by using PCR amplification. Our results are shown in Figure 3. As expected, CRP in the presence of cAMP bends all three sets of DNA fragments. The mobility of CRP−DNA complexes is position-dependent, with the highest mobility for CRP bound to either end of the DNA fragments and the lowest mobility for CRP bound to the center of the DNA fragments (Figure 3). The CRP-induced DNA bending angles were estimated to be ~90° for all three DNA fragments (Table 3), which are consistent with published data (*27*). We also plotted the relative mobility of the CRP−DNA complexes versus the position of the CRP binding sites of the three DNA fragments, which resulted in the extrapolated bending locus at the center of the CRP binding

site (Figure 3D). These results are also consistent with the published results (*27*). These studies of CRP-induced DNA bending suggest that pBendAT can be used to study DNA bending induced by sequence-specific DNA binding proteins.

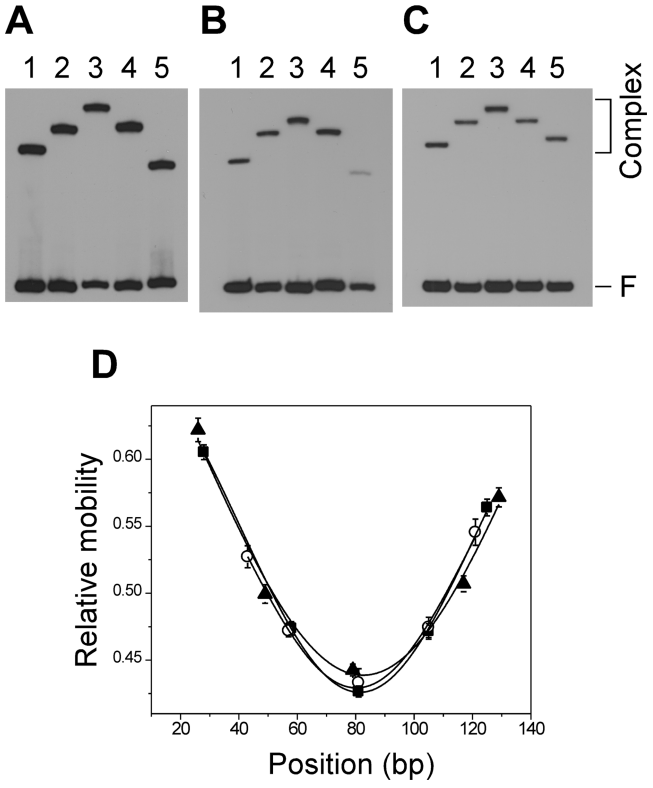

FIGURE 3: DNA bending induced by CRP. DNA bending assays were conducted as described in Materials and Methods. After the binding of CRP to the permutated DNA fragments in the presence of 20 μM cAMP, an 8% polyacrylamide gel was used to separate the bound and free DNA fragments. The autoradiograms of ^{32}P-labeled DNA fragments are shown. The DNA fragments in the bottom of the gels are free DNA, and those in the top part are protein−DNA complexes. F denotes the free DNA, and complex denotes the protein−DNA complex. (A) *lac P1* promoter's CRP fragments produced by digestion of plasmid pBend2-CRP with restriction enzymes MluI, NheI, EcoRV, SspI, and BamHI in lanes 1−5, respectively. (B) *lac P1* promoter's CRP fragments produced by digestion of plasmid pBendAT-CRP with a pair of restriction enzymes: BspEI and EagI, KpnI and SphI, NheI and AvrII, BamHI and BglII, and SacI and PstI for lanes 1−5, respectively. (C) *lac P1* promoter's CRP fragments produced using PCR amplification as described in the legend of Figure 2. (D) Plot of the relative mobility of CRP−DNA complexes vs the location of the CRP binding site within the 159 bp fragment of pBend2 or the 149 bp fragment of pBendAT: bending data using the *lac P1* promoter CRP fragments generated by restriction digestion of pBend2-CRP (■), restriction digestion of pBendAT-CRP (▲), and PCR amplification of pBendAT-CRP (○). The standard deviations are also shown.

To study HMGA2-induced DNA bending, we cloned three different HMGA2 binding sites, SELEX1, SELEX2, and PRDII, into pBendAT to yield pBendAT-SELEX1, pBendAT-SELEX2, and pBendAT-PRDII, respectively (Table 2). We determined the binding stoichimtry and the DNA binding constant of HMGA2 binding to these three DNA binding sites (the NheI−AvrII fragments of the pBendAT derivatives) using an electrophoretic mobility shift assay (EMSA). Our results are shown in Figure 4 and Table 3. In these EMSA experiments, only one shifted band was observed, indicating that the DNA fragments contain only one DNA binding site for HMGA2 (*21*). Interestingly, the DNA binding constants (K) of HMGA2 binding to SELEX1 and SELEX2 were determined to be $(5.2 \pm 3.0) \times 10^7$ and $(3.9 \pm 1.9) \times 10^7$ M^{-1}, respectively, 10-fold higher than the K of HMGA2 binding to PRDII [$(3.1 \pm 1.3) \times 10^6$ M^{-1}]. These results suggest that SELEX1 and SELEX2 are indeed the preferred DNA binding sequences of HMGA2 (*21*). Our results are summarized in Table 3, which are consistent with the previously published results (*21*, *28*). We next determined HMGA2-induced DNA bending for these DNA binding sites using the DNA fragments generated from pBendAT-SELEX1, pBendAT-SELEX2, and pBendAT-PRDII by PCR amplification. Our results are shown in Figure 5 and Table 3. The mobility of the five free DNA fragments is identical, indicating no intrinsic curvature for the HMGA2 binding sites, SELEX1, SELEX2, and PRDII. The binding of HMGA2 to these binding sites induces a small bend in all three DNA fragments (Figure 5 and Table 3). Similar to CRP binding to its binding site, the mobility of HMGA2−DNA complexes is also position-dependent, with the highest mobility for HMGA2 bound to either end of the DNA fragments and the lowest mobility for HMGA2 bound to the center of the DNA fragments (Figure 5). The DNA bending angles were calculated to be $34.2 \pm 2.3°$, $33.5 \pm 1.7°$, and $35.4 \pm 1.8°$ for SELEX1, SELEX2, and PRDII, respectively (Table 3). The relative mobility of the HMGA2−DNA complexes was plotted against the position of the HMGA2 binding sites of the three DNA fragments, which resulted in the extrapolated bending locus at the center of the HMGA2 binding site (Figure 5C,D). Similar results were also obtained using DNA fragments generated with restriction enzyme digestion (data not shown). Since HMGA contains three AT hook DNA binding domains specifically binding to the minor groove of AT-rich DNA sequences, the induced DNA bending may be caused by the neutralization of the negative charges in the minor groove of the two AT-rich sequences in the HMGA2 binding sites [unbalanced inter-phosphate repulsion (*22*)]. In this case, the HMGA2-induced DNA

Table 3: DNA Bending Angles and Binding Constants of HMGA2 and CRP

DNA binding protein	DNA binding site	DNA binding constant (M^{-1})	DNA bending angle (deg)
CRP	CRP binding site	$(2.8 \pm 1.1) \times 10^9$	89.9 ± 0.8^a
CRP	CRP binding site	N/A	89.4 ± 1.0^b
CRP	CRP binding site	N/A	90.3 ± 0.9^c
HMGA2	SELEX1	$(5.2^d \pm 3.0) \times 10^7$	34.2 ± 2.3^d
HMGA2	SELEX2	$(3.9^d \pm 1.9) \times 10^7$	33.5 ± 1.7^d
HMGA2	PRDII	$(3.1^d \pm 1.3) \times 10^6$	35.4 ± 1.8^d

[a]CRP-induced DNA bending angle were estimated by using DNA fragments produced by restriction digestion of pBend2-CRP. [b]CRP-induced DNA bending angle were estimated by using DNA fragments produced by restriction digestion of pBendAT-CRP. [c]CRP-induced DNA bending angle were estimated by using DNA fragments produced by PCR amplification of pBendAT-CRP. [d]HMGA2-induced DNA bending angles and DNA binding constants were determined as described in Materials and Methods. The DNA fragments of identical length were produced by PCR amplification of pBendAT derivatives.

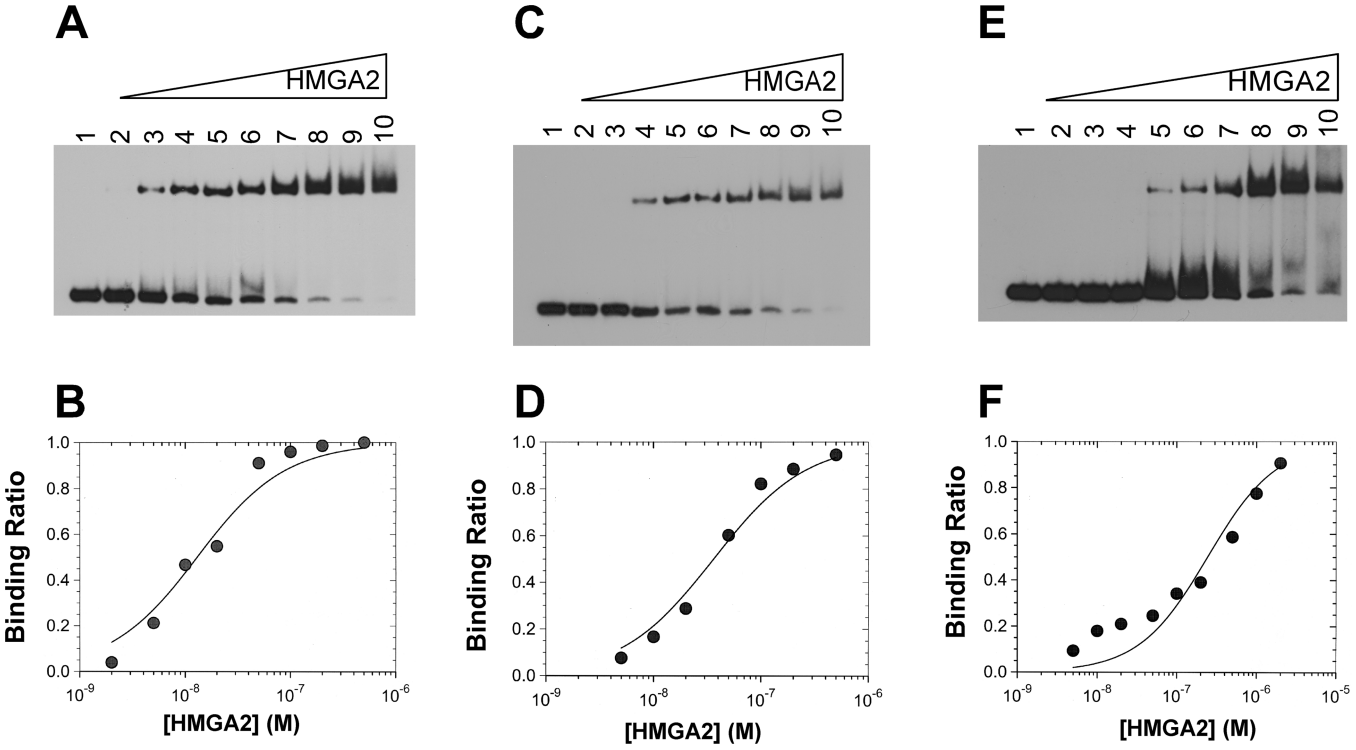

FIGURE 4: Quantitative EMSA experiments for determining the DNA binding constants for binding of HMGA2 to SELEX1 (A and B), SELEX2 (C and D), and PRDII (E and F) (the NheI−AvrII fragment of the pBendAT derivatives). ^{32}P-labeled HMGA2 binding fragments (0.2 nM) were incubated with increasing concentrations of HMGA2 in 50 μL of 1× EMSA binding buffer containing 20 mM Tris-HCl (pH 8.0), 200 mM NaCl, 0.5 mM EDTA, 1 mM DTT, 0.5 mM $MgCl_2$, and 5% glycerol. EMSA experiments were performed as described in Materials and Methods. The autoradiograms of ^{32}P-labeled FL-SELEX1 are shown. Lane 1 contained the free DNA fragment. In addition to the DNA fragment, lanes 2−10 also contained 1, 2, 5, 10, 20, 50, 100, 200, and 500 nM HMGA2, respectively. (B, D, and F) Quantification analysis of the binding data from the EMSA experiments. The bound ratio of DNA was plotted vs the protein concentration. The curves are generated from fitting the data to eq 2 as described in Materials and Methods.

bend (~35°) may result from two 17° DNA bends that occur in the AT-rich sequences and is toward the minor groove. This analysis is consistent with the phasing analyses published previously (*23*).

The results presented here have great biological implications. The HMGA proteins, including HMGA2, are chromatin architectural factors that participate in many nuclear processes, such as transcription regulation, DNA repair, chromatin remodeling, RNA processing, and others (*29*). The critical role of HMGA proteins is to organize the assembly of the regulatory nucleoprotein complexes for these biological functions. For instance, the first step of the assembly of a functional enhanceosome of human β-interferon (hINF-β) is to recruit HMGA1a into the two AT-rich regions of the hINF-β promoter [two molecules of HMGA1a bind to four sites within the promoter region PRDII and PRDIV (*30*)]. Binding of HMGA1a to the enhancer changes the DNA conformation, i.e., DNA bending, allowing cooperative recruitment of other transcription factors such as NF-κB, ATF-2/c-JUN, and IRFs that together with HMGA1a assemble into a highly stable nucleoprotein complex enhanceosome. The enhanceosome then provides a correct surface for other transcription activators cooperating with the RNA polymerase II holoenzyme to initiate transcription (*31*). Since it was previously demonstrated that HMGA2 also binds to the promoter fragment containing the PRDII element and enhances transcriptional activation of the hINF-β gene (*24*, *32*), HMGA2-induced DNA bending presented in this paper provides direct evidence of the DNA conformational change of the AT-rich regulatory elements in the enhanceosome upon binding to HMGA proteins to promote these transcriptional activities.

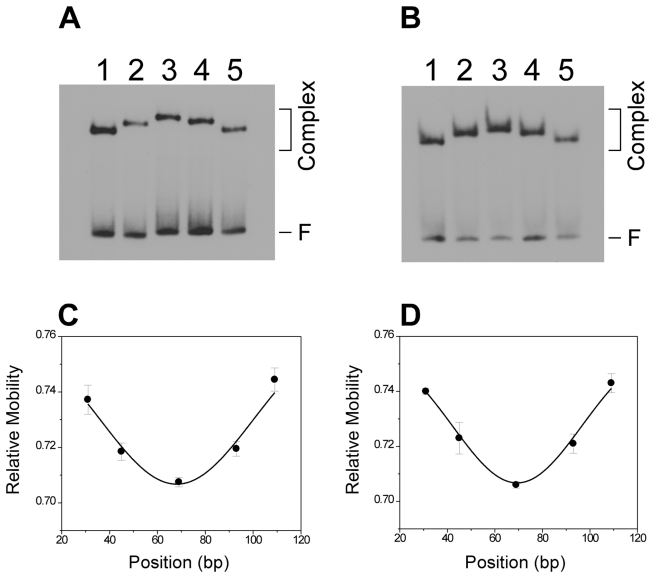

FIGURE 5: DNA bending induced by HMGA2. DNA bending assays were conducted as described in Materials and Methods. After the binding of HMGA2 to the DNA fragments of identical size generated from pBendAT-SELEX1 (A) or pBendAT-SELEX2 (B) by PCR amplification, an 8% polyacrylaimde gel was used to separate the bound and free DNA fragments. The autoradiograms of ^{32}P-labeled DNA fragments are shown. The DNA fragments in the bottom of the gels are free DNA, and those in the top part are protein−DNA complexes. F denotes the free DNA, and complex denotes the protein−DNA complex. (C and D) Plots of the relative mobility of HMGA2−DNA complexes vs the location of the HMGA2 binding site within the 135 bp fragment for pBendAT-SELEX1 and pBendAT-SELEX2, respectively. The standard deviations are also shown.

CONCLUSION

In this paper, we have constructed a pBendAT plasmid to study DNA bending by the mammalian high-mobility group protein AT hook 2 (HMGA2). pBendAT carries a 230 bp DNA fragment that contains five pairs of restriction enzyme recognition sites that can be used to generate a set of short DNA fragments of identical size to study protein-induced DNA bending. This set of DNA fragments can also be produced by PCR amplification. Since the 230 bp DNA fragments do not contain three consecutive AT base pairs, pBendAT is particularly suitable for the study of DNA bending induced by the DNA binding proteins recognizing AT-rich DNA sequences. Indeed, using pBendAT, we found that HMGA2 induces a small bend in all three binding sequences, i.e., SELEX1, SELEX2, and PRDII.

SUPPORTING INFORMATION AVAILABLE

Map of pBend2 (Figure S1) and EMSA experiments aimed at examining the binding of HMGA2 to the EcoRV fragments generated from digestion of pBend2-SELEX1 and pBend2-PRDII using restriction enzyme EcoRV (Figure S2). This material is available free of charge via the Internet at http://pubs.acs.org.

REFERENCES

1. Zhou, X., Benson, K. F., Ashar, H. R., and Chada, K. (1995) Mutation responsible for the mouse pygmy phenotype in the developmentally regulated factor HMGI-C. *Nature 376*, 771–774.
2. Anand, A., and Chada, K. (2000) In vivo modulation of HMGIC reduces obesity. *Nat. Genet. 24*, 377–380.
3. Reeves, R. (2003) HMGA proteins: Flexibility finds a nuclear niche? *Biochem. Cell Biol. 81*, 185–195.
4. Reeves, R., and Beckerbauer, L. M. (2003) HMGA proteins as therapeutic drug targets. *Prog. Cell Cycle Res. 5*, 279–286.
5. Klotzbucher, M., Wasserfall, A., and Fuhrmann, U. (1999) Misexpression of wild-type and truncated isoforms of the high-mobility group I proteins HMGI-C and HMGI(Y) in uterine leiomyomas. *Am. J. Pathol. 155*, 1535–1542.
6. Ashar, H. R., Fejzo, M. S., Tkachenko, A., Zhou, X., Fletcher, J. A., Weremowicz, S., Morton, C. C., and Chada, K. (1995) Disruption of the architectural factor HMGI-C: DNA-binding AT hook motifs fused in lipomas to distinct transcriptional regulatory domains. *Cell 82*, 57–65.
7. Schoenmakers, E. F., Wanschura, S., Mols, R., Bullerdiek, J., Van den, B. H., and Van de Ven, W. J. (1995) Recurrent rearrangements in the high mobility group protein gene, HMGI-C, in benign mesenchymal tumours. *Nat. Genet. 10*, 436–444.
8. Kazmierczak, B., Rosigkeit, J., Wanschura, S., Meyer-Bolte, K., Van de Ven, W. J., Kayser, K., Krieghoff, B., Kastendiek, H., Bartnitzke, S., and Bullerdiek, J. (1996) HMGI-C rearrangements as the molecular basis for the majority of pulmonary chondroid hamartomas: A survey of 30 tumors. *Oncogene 12*, 515–521.
9. Sarhadi, V. K., Wikman, H., Salmenkivi, K., Kuosma, E., Sioris, T., Salo, J., Karjalainen, A., Knuutila, S., and Anttila, S. (2006) Increased expression of high mobility group A proteins in lung cancer. *J. Pathol. 209*, 206–212.
10. Chang, Z. G., Yang, L. Y., Wang, W., Peng, J. X., Huang, G. W., Tao, Y. M., and Ding, X. (2005) Determination of high mobility group A1 (HMGA1) expression in hepatocellular carcinoma: A potential prognostic marker. *Dig. Dis. Sci. 50*, 1764–1770.
11. Rogalla, P., Drechsler, K., Schroder-Babo, W., Eberhardt, K., and Bullerdiek, J. (1998) HMGIC expression patterns in non-small lung cancer and surrounding tissue. *Anticancer Res. 18*, 3327–3330.
12. Rommel, B., Rogalla, P., Jox, A., Kalle, C. V., Kazmierczak, B., Wolf, J., and Bullerdiek, J. (1997) HMGI-C, a member of the high mobility group family of proteins, is expressed in hematopoietic stem cells and in leukemic cells. *Leuk. Lymphoma 26*, 603–607.
13. Kottickal, L. V., Sarada, B., Ashar, H., Chada, K., and Nagarajan, L. (1998) Preferential expression of HMGI-C isoforms lacking the acidic carboxy terminal in human leukemia. *Biochem. Biophys. Res. Commun. 242*, 452–456.
14. Abe, N., Watanabe, T., Sugiyama, M., Uchimura, H., Chiappetta, G., Fusco, A., and Atomi, Y. (1999) Determination of high mobility group I(Y) expression level in colorectal neoplasias: A potential diagnostic marker. *Cancer Res. 59*, 1169–1174.
15. Meyer, B., Loeschke, S., Schultze, A., Weigel, T., Sandkamp, M., Goldmann, T., Vollmer, E., and Bullerdiek, J. (2007) HMGA2 overexpression in non-small cell lung cancer. *Mol. Carcinog. 46*, 503–511.
16. Fusco, A., and Fedele, M. (2007) Roles of HMGA proteins in cancer. *Nat. Rev. Cancer 7*, 899–910.
17. Miao, Y., Cui, T., Leng, F., and Wilson, W. D. (2008) Inhibition of high-mobility-group A2 protein binding to DNA by netropsin: A biosensor-surface plasmon resonance assay. *Anal. Biochem. 374*, 7–15.
18. Huth, J. R., Bewley, C. A., Nissen, M. S., Evans, J. N., Reeves, R., Gronenborn, A. M., and Clore, G. M. (1997) The solution structure of an HMG-I(Y)-DNA complex defines a new architectural minor groove binding motif. *Nat. Struct. Biol. 4*, 657–665.
19. Cui, T., Wei, S., Brew, K., and Leng, F. (2005) Energetics of binding the mammalian high mobility group protein HMGA2 to poly(dA-dT)2 and poly(dA)-poly(dT). *J. Mol. Biol. 352*, 629–645.
20. Maher, J. F., and Nathans, D. (1996) Multivalent DNA-binding properties of the HMG-1 proteins. *Proc. Natl. Acad. Sci. U.S.A. 93*, 6716–6720.
21. Cui, T., and Leng, F. (2007) Specific recognition of AT-rich DNA sequences by the mammalian high mobility group protein AT-hook 2: A SELEX study. *Biochemistry 46*, 13059–13066.
22. Maher, L. J., III (1998) Mechanisms of DNA bending. *Curr. Opin. Chem. Biol. 2*, 688–694.
23. Falvo, J. V., Thanos, D., and Maniatis, T. (1995) Reversal of intrinsic DNA bends in the IFN β gene enhancer by transcription factors and the architectural protein HMG I(Y). *Cell 83*, 1101–1111.
24. Mantovani, F., Covaceuszach, S., Rustighi, A., Sgarra, R., Heath, C., Goodwin, G. H., and Manfioletti, G. (1998) NF-κB mediated transcriptional activation is enhanced by the architectural factor HMGI-C. *Nucleic Acids Res. 26*, 1433–1439.
25. Cui, T., Joynt, S., Morillo, V., Baez, M., Hua, Z., Wang, X., and Leng, F. (2007) Large scale preparation of the mammalian high mobility group protein A2 for biophysical studies. *Protein Pept. Lett. 14*, 87–91.
26. Thompson, J. F., and Landy, A. (1988) Empirical estimation of protein-induced DNA bending angles: Applications to λ site-specific recombination complexes. *Nucleic Acids Res. 16*, 9687–9705.
27. Kim, J., Zwieb, C., Wu, C., and Adhya, S. (1989) Bending of DNA by gene-regulatory proteins: Construction and use of a DNA bending vector. *Gene 85*, 15–23.
28. Joynt, S., Morillo, V., and Leng, F. (2009) Binding the mammalian high mobility group protein AT-hook 2 to AT-rich deoxyoligonucleotides: Enthalpy-entropy compensation. *Biophys. J. 96*, 4144–4152.
29. Sgarra, R., Zammitti, S., Lo Sardo, A., Maurizio, E., Arnoldo, L., Pegoraro, S., Giancotti, V., and Manfioletti, G. (2009) HMGA molecular network: From transcriptional regulation to chromatin remodeling. *Biochim. Biophys. Acta* (in press).
30. Thanos, D., and Maniatis, T. (1992) The high mobility group protein HMG I(Y) is required for NF-κB-dependent virus induction of the human IFN-β gene. *Cell 71*, 777–789.
31. Thanos, D., and Maniatis, T. (1995) Virus induction of human IFN β gene expression requires the assembly of an enhanceosome. *Cell 83*, 1091–1100.
32. Schwanbeck, R., Manfioletti, G., and Wisniewski, J. R. (2000) Architecture of high mobility group protein I-C·.DNA complex and its perturbation upon phosphorylation by Cdc2 kinase. *J. Biol. Chem. 275*, 1793–1801.